J Solid State Electrochem (2012) 16:1099–1104
DOI 10.1007/s10008-011-1501-x

ORIGINAL PAPER

Electrocatalytic oxidation of glucose on nanoporous gold membranes

Qianqian Li · Songzhi Cui · Xiuling Yan

Received: 1 February 2011 / Revised: 30 June 2011 / Accepted: 3 July 2011 / Published online: 16 July 2011

Abstract With characteristic of structural integrity and high surface area, nanoporous gold (NPG) prepared by dealloying method is proposed to be a highly sensitive catalyst for glucose electrooxidation. It can be found that a-NPG which obtained by electrochemical corrosion method has the highest sensitivity for glucose electrooxidation among the three studied samples. Under alkaline conditions, the catalytic current density of a-NPG is over 1.5 times and 17 times higher than that of f-NPG (prepared by free corrosion) and poly-Au electrode, respectively. Using a-NPG sample for glucose detection, the obtained minimum sensible concentration are 413 nM in alkaline media and 1 μM in neutral solutions. The a-NPG electrode also shows stable recovery and reproducibility characteristics. These results indicate that NPG may work as an efficient electrode material for electrochemical sensors and a promising catalyst for alkaline glucose fuel cells.

Keywords Glucose oxidation · Nanoporous gold · Electrocatalysis · Detection · Nonenzymatic sensor

Introduction

Electrocatalytic oxidation of glucose, as a key reaction in the fields of sensors [25, 29] and fuel cells [13, 19], has been widely investigated during the past decades. Nanomaterials with special surface structures and properties provide great opportunities for this oxidation reaction [4]. Besides the widely used nanoparticles [30, 33, 34], the reported nanostructures also include porous materials [9, 15, 22]. Due to the three-dimensional and continuous pore channels, porous metallic materials possess excellent performances for catalysis, sensing, and biotechnology [6, 8, 10, 18]. Among various porous metallic materials, the nanoporous gold (NPG), a unique class of functional materials for catalytic applications [21, 27, 28], have been extensively studied since Au would not be self-poisoned [14, 24, 26], and its activity could be regenerated after removing the oxidation products on the surface [2, 3]. Although there are so many approaches to achieve this desired material [16, 17], the simple dealloying process [7] represents a facile method to fabricate NPG with extremely clean surface, which is a well-known significant factor for electrochemistry.

As have been proved in previous works, NPG shows superior activity toward a series of important electrochemical reaction including methanol oxidation [12, 32], formic acid oxidation [11], thus are regarded as promising electrocatalysts in glucose electrooxidation. Recently, Ma et al. prepared nanoporous Au–Ag alloy with different Ag content, and they found the existence of a tiny amount of silver can obviously enhanced catalytic activity for the electrooxidation of glucose [23]. In this work, our interest is focused on the use of NPG membranes in glucose detection and further in nonenzymatic biosensors. Systematical studies demonstrate that NPG shows much higher electrocatalytic activity and sensitivity toward glucose oxidation in alkaline and neutral solutions than polycrystalline gold. Additionally, glucose detection under physiological condition is also monitored. The results indicate that NPG is a

Q. Li · S. Cui · X. Yan
School of Chemistry and Chemical Engineering,
Shandong University,
Jinan 250100, China

X. Yan (✉)
School of Chemistry and Bioscience, Yili Normal University,
Xinjiang 835000, China
e-mail: xiuling1212@gmail.com

potential material to be used in nonenzymatic glucose biosensor.

Experimental

Reagents and apparatus

All chemicals were of analytical grade and used as purchased without further purification. D-Glucose, NaOH, HNO_3 (67%), $Na_2HPO_4{\cdot}12H_2O$, and $NaH_2PO_4{\cdot}2H_2O$ were obtained from Sinopharm Chemical Reagent Co., Ltd. Ultra pure water (18.2 MΩ) was used throughout the experiments, and 0.1 M phosphate buffer solutions (PBS) were prepared with pH 7.4. Au/Ag alloy (50:50, wt.%) leaves with thickness of 100 nm (Sepp Leaf Products, New York) were used for NPG fabrication. The surface structure of NPG was observed use JSM-6700F SEM. All electrochemical measurements were performed at room temperature in a three-electrode electrochemical cell with a CHI 760C electrochemical workstation (Shanghai). Saturated calomel electrode (SCE) was selected as reference electrode in all electrochemical measurements and a pure Pt foil as the counter electrode. Both NaOH and PBS solutions were purged with high pure nitrogen (99.999%) for 20 min prior to measuring.

Preparation of NPG electrodes

NPG with 35-nm pore size was made by dealloying commercial 12-carat white gold ($Au_{50}Ag_{50}$ wt.%) membrane in concentrated (67%) nitric acid (free corrosion) for 30 min at 303 K (mark as f-NPG). The NPG with 12-nm pore size was obtained by electrochemical dealloying under anodic potential (600 mV) for 25 s at 303 K on a CHI 760C (mark as a-NPG). Subsequently, these two NPG samples were immediately transferred to ultra-pure water and repeatedly washed to remove Ag^+ and NO_3^-. Then, the membranes were affixed onto a clean glassy carbon electrode and fixed with 2 μL dilute Nafion solution (0.5 wt.%). The as-prepared NPG electrodes were dried at room temperature before measuring.

Results and discussion

Surface structure of the NPG

Figure 1 shows the SEM images of NPG samples, which exhibits unique structure of free-supporting, three-dimensional, bi-continuous, and highly porous network with even pore size. Figure 1a shows NPG sample prepared under free corrosion conditions. Dealloying Au/Ag foil is a competition process between silver atoms dissolution which induced surface roughening and gold atoms diffusion which induced surface smoothing. This competition makes the three-dimensional porous structure. The sample obtained under this condition is named f-NPG with pore size about 35 nm. While in Fig. 1b, instead of free corrosion, electrochemical dealloying technique is employed to control the pore size [27]. The sample obtained under this condition is named a-NPG with pore size about 12 nm (Fig. 1b).

Electrocatalytic properties of NPG for glucose oxidation in alkaline media

The f-NPG and a-NPG samples were further characterized by means of cyclic voltammetries (CV) tests in 0.1 M NaOH aqueous solution with (curve b) and without (curve a) 10 mM glucose solution (Fig. 2). Poly-Au electrode was also used here for comparison. The detailed description of

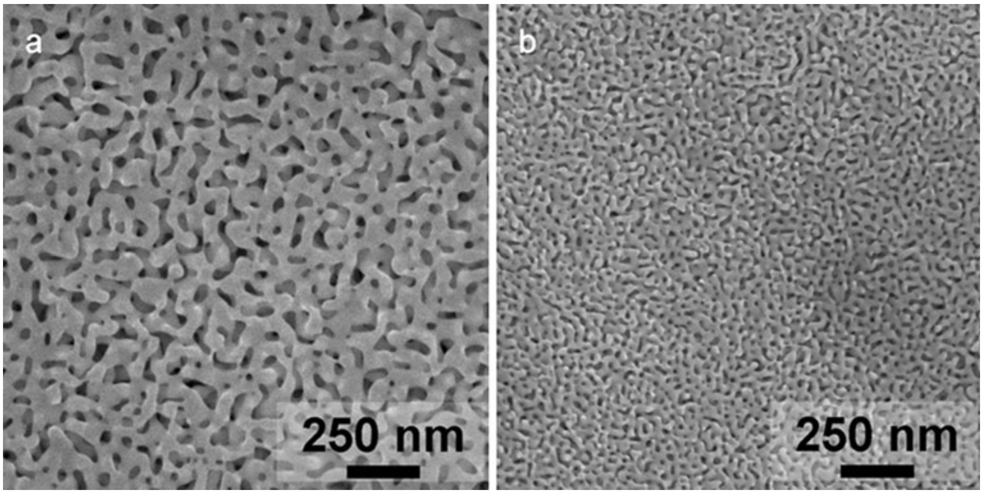

Fig. 1 SEM images of f-NPG (**a**) and a-NPG (**b**) samples with different pore sizes

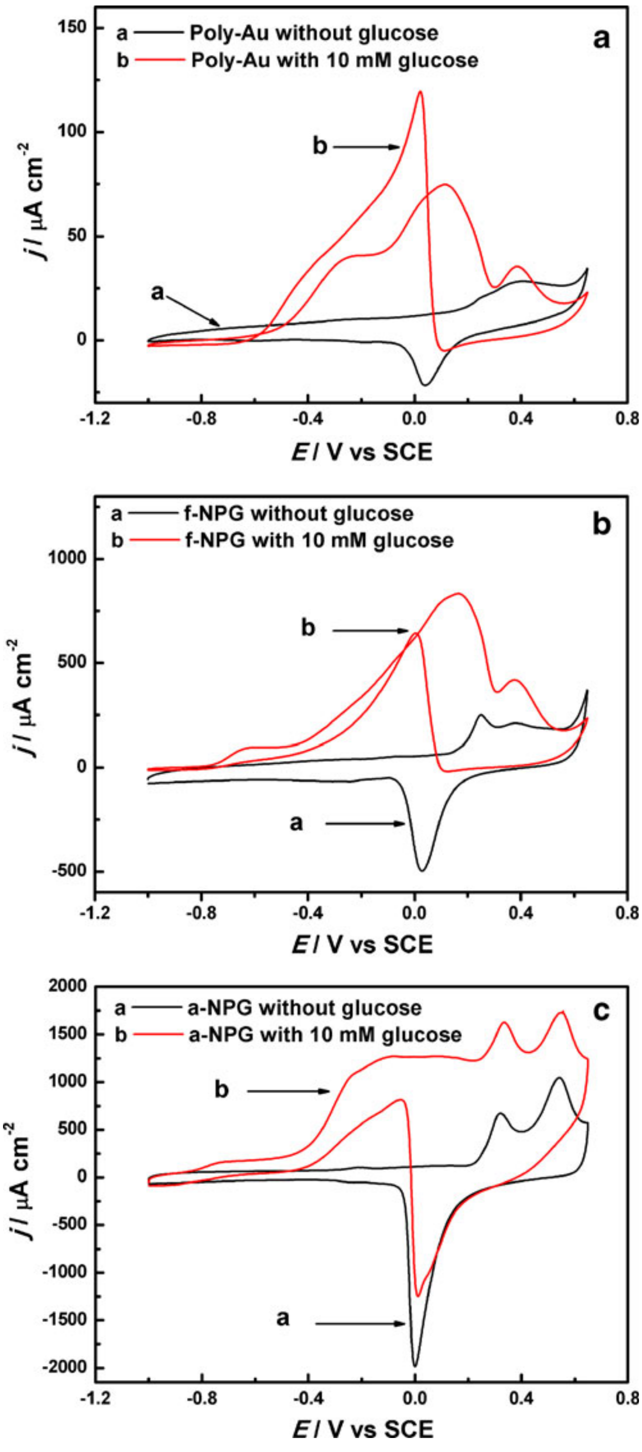

Fig. 2 Cyclic voltammograms (CVs) of different electrodes in a N_2-satutated 0.1 M NaOH solutions (curve *a*) and 0.1 M NaOH+10 mM glucose (curve *b*) at 293 K. Scan rate was 20 mV s^{-1}

glucose oxidation peaks in Fig. 2 had been listed in Table 1. During the positive scan, the peaks in the potential region between ~−1.0 and −0.1 V (column 1, Table 1) were the results of glucose oxidation on active Au surface, producing a layer of adsorbed glucose intermediates on electrode surface [5]. These intermediate species were then oxidized at a positive potential (column 2, Table 1) [1]. During the negative scan, the glucose was re-oxidized on the partially oxidized Au surface followed by the partial reduction of surface gold oxides, giving an extend oxidation peak (column 4, Table 1). Meanwhile, compared with poly-Au and f-NPG, the obvious negative shift of the onset potential and enhancement of peak current density (column 3, Table 1) of the a-NPG indicated a superior catalytic activity toward glucose oxidation [23].

The chronoamperometric (CA) measurements were carried out at −0.2 V for 300 s on these three catalysts in 0.1 M NaOH solution containing 10 mM glucose. The results in Fig. 3 also supported above findings that a-NPG was the most active catalyst among these three samples. The current became relatively stable after a sharp drop during the first few minutes due to double layer charge and discharge. With the reaction going on, the adsorbed intermediate species known as the competitor with the glucose adsorption rapidly formed and occupied the active surface sites to reach dynamic balance. This proved that the active surface area of a catalyst material directly affected the catalytic capability toward oxidation of glucose.

The a-NPG possessed a higher number of electrochemically active surfaces than poly-Au, which implied that the structure of a-NPG is beneficial for more glucose to achieve active sites. Linear sweep voltammetry was carried out to integrate the anodic peak charges for glucose oxidation at different scan rates as shown in Fig. 4. Q_v represented the integrated charge of the anodic peak for glucose oxidation a different scan rates. Q_m represented the charge obtained at the scan rate of 2 mV s^{-1}. It demonstrated that the Q_v/Q_m ratios of both electrodes decreased with the increase of scan rate. However, the decrease on a-NPG was slower than poly-Au, indicating that the oxidation of glucose on a-NPG catalyst was controlled by activation polarization at lower scan rates because the nanoporous structure provided more active sites for glucose oxidation. This was further proven by plotting the peak current density against the square root of the scan rate as shown in the inset of Fig. 4. It showed a straight line on poly-Au electrode while a-NPG deviated from the line, which can be attributed to the gradient concentration effect in the nanoporous structure of a-NPG.

To evaluate the catalytic performance of a-NPG catalyst in alkaline solution, the amperometric response toward the oxidation of glucose was tested on rotating disk electrode (1,600 rpm). Figure 5 shows the typical steady-state current time response of the rotated a-NPG electrode. A quick response (response time less than 3 s) was observed during the successive glucose (1 μM) injection under a constant applied potential of −0.2 V (vs. SCE). The calibration plot for glucose current vs. concentration is linear in the range from 1 μM to 10 μM with a slope of 0.32242 μA μM^{-1}.

Table 1 A detailed description of glucose oxidation peaks in Fig. 2

Electrode	E_{p1}	E_{p2}	I_{p2}	E_n
Poly-Au	−0.6~−0.16 V	−0.15~0.3 V	74.8 mA cm^{-2}	−0.6~0.1 V
f-NPG	−0.8~−0.5 V	−0.5~0.3 V	831.2 mA cm^{-}	−0.8~0.1 V
a-NPG	−0.9~−0.5 V	−0.5~−0.24 V	1270.2 mA cm^{-2}	−0.9~−0.01 V

E_{p1} the potential of first oxidation peak during positive scan

E_{p2} the potential of second oxidation peak during positive scan

I_{p2} the current density of the second oxidation peak

E_n the potential of oxidation peak during negative scan

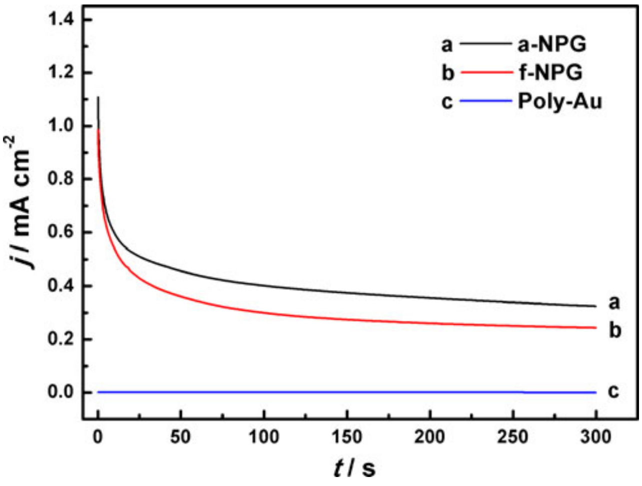

Fig. 3 Chronoamperometric (CA) measurements carried out on poly-Au, f-NPG, and a-NPG electrodes at −0.2 V for 300 s

According to the equation: C_L=3 S_d/k [31], where C_L is the detection limit, S_d (0.09439 μA) is the standard deviation of the blank response under rotating conditions (1,600 rpm) and k is the slope of the calibration plot, the detection limit of glucose in alkaline solution was calculated as low as 413 nM. This proves that NPG is highly sensitive to oxidation of glucose.

Electrocatalytic properties of a-NPG for glucose oxidation in neutral media

The catalytic performance of a-NPG catalyst in neutral media was tested on rotating disk electrode (1,600 rpm) in 0.1 M pH 7.4 PBS. Figure 6a showed the CVs of a-NPG in PBS with (curve b) and without (curve a) 10 mM glucose at 20 mV s^{-1}. The onset potential of glucose oxidation was about −0.4 V and an obvious oxidation wave

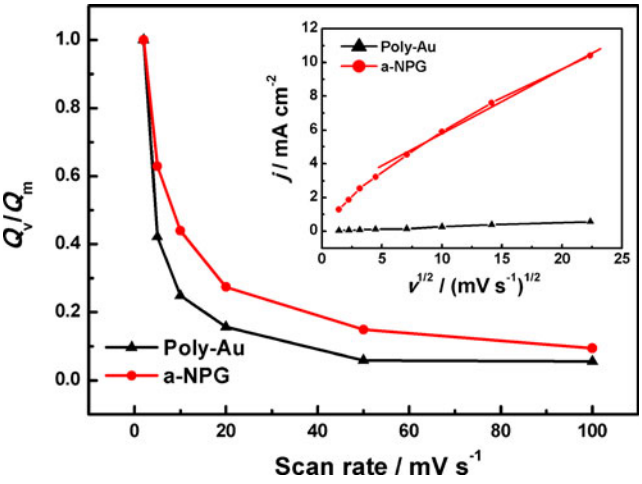

Fig. 4 Curve of normalized charge of anodic peak of glucose oxidation on poly-Au and a-NPG electrodes against the scan rate. *Inset* presents the plots of the peak current density against the square root of the scan rate for tow electrodes

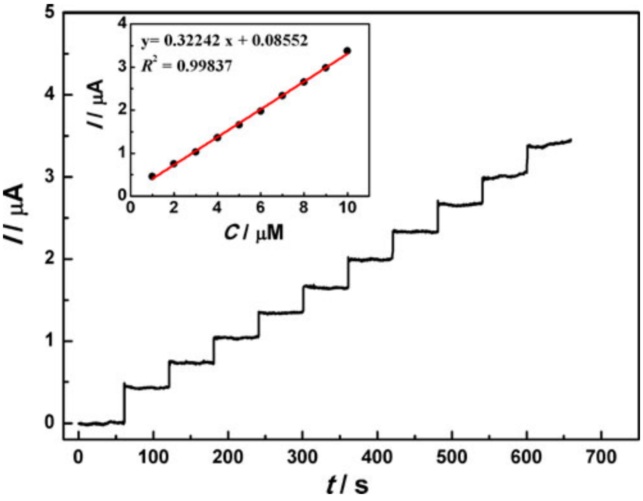

Fig. 5 Current-time record of a-NPG affixed onto rotating disk electrode (1,600 rpm) by successively injection 1 μM glucose into 0.1 M NaOH solution at a regular interval time of 60 s. Applied potential is −0.2 V. *Inset*: the corresponding calibration plot of glucose oxidation current vs. concentration

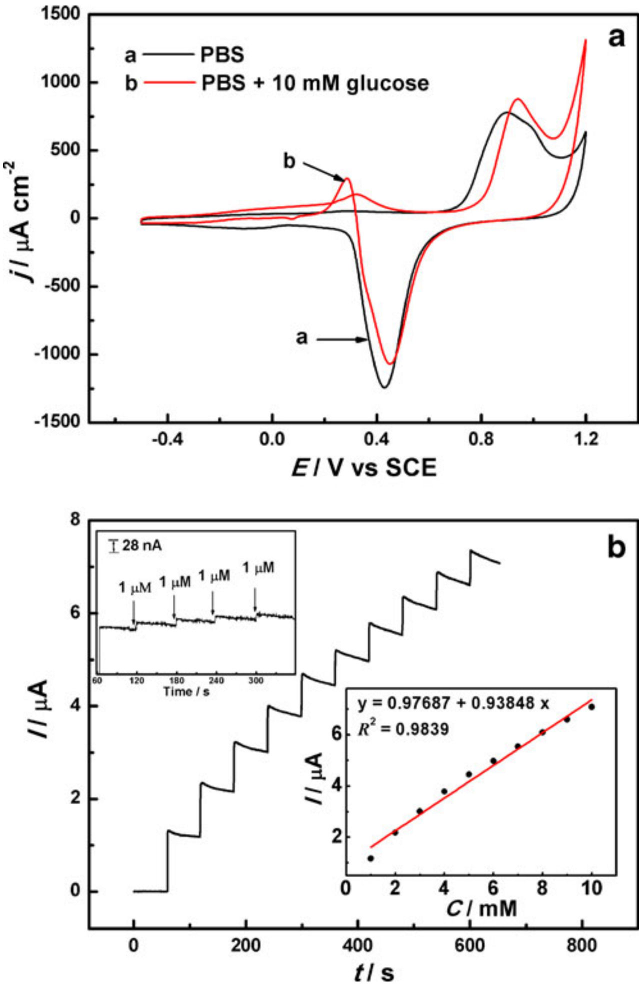

Fig. 6 **a** CVs of a-NPG in N_2-satutated 0.1 M PBS (pH 7.4) (curve *b*) and 0.1 M PBS (pH 7.4)+10 mM glucose (curve *a*). The potential scan rate is 20 mV s^{-1}. **b** Current-time record of a-NPG affixed onto rotating disk electrode (1,600 rpm) by successively injection 1 mM glucose into 0.1 M PBS (pH 7.4) at a regular interval time of 60 s. Applied potential is 0.3 V. *Upper left inset*: the current response of a-NPG towards 1 μM glucose; *lower right inset*: the corresponding calibration plot of glucose oxidation current vs. concentration

was observed at about 0.32 V in positive potential scan process and the re-oxidation peak in negative scan process could be found at about 0.29 V. Therefore, the selected potential for amperometric measurement on a-NPG towards glucose oxidation is 0.3 V in neutral media (Fig. 6b). The linear dependence (R^2=0.9839) of the amperometric response can be seen in the range of 0~10 mM. The low detection limit of 1 μM makes a great possibility for a-NPG catalyst material to be used as enzyme-free glucose sensor in clinical condition.

As we all know, though the real clinical samples normally contains some other species which has similar electroactivities with glucose, such as AA, urea, and sucrose, the physiological level of glucose is much higher than that of those mentioned matters. So, the anti-interferents study of a-NPG was performed in 0.1 M PBS (pH 7.4) with successively injected 5 mM glucose, then 0.1 mM AA, urea, and sucrose which were used as the co-exist samples to disturb the current response of glucose. From Fig. 7a, we can clearly see that not only the stability but also the linear of the amperometric response were not affected by urea and sucrose. The wave on the stability induced by AA was not enough to interfering the detection of glucose that this could be neglected. As shown in Fig. 7b, the recovery characteristics of this electrode toward

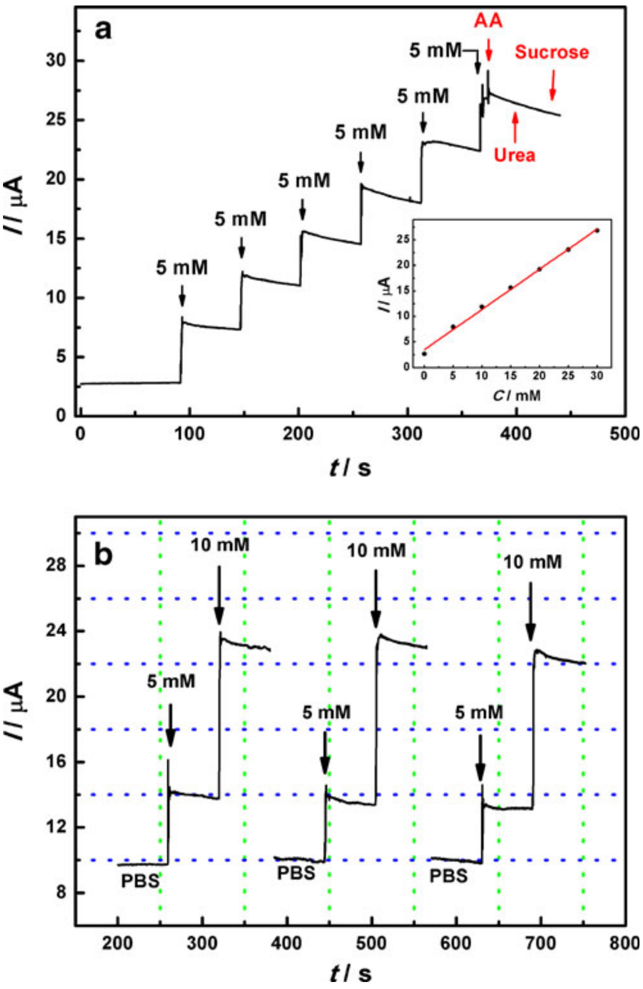

Fig. 7 **a** Current-time record of a-NPG affixed onto rotating disk electrode (1,600 rpm) by successively injection 5 mM glucose and 0.1 mM AA, urea, and sucrose into 0.1 M PBS (pH 7.4) at a regular interval time of 60 s; **b** The recovery characteristics of the a-NPG with 0, 5, 10 mM glucose concentration. Applied potential is 0.3 V

Table 2 The data of reproducibility on a-NPG electrodes

Electrode number	1	2	3	4	5	6
Current density, μA cm^{-2}	4.2	4.8	4.6	3.9	4.3	4.8

different concentrations of glucose (0, 5, and 10 mM) were illustrated by current-time records. The tests were carried out by successive injections of glucose at 0 (i.e., PBS without glucose), 5, and 10 mM at 60-s intervals, and then the experiment was repeated using the same electrode. For the states of 0, 5, and 10 mM glucose, the corresponding recovery rates were calculated to be 95%, 90.8%, and 95.6%.

To be used in glucose sensors, it is necessary to evaluate whether all the a-NPG samples formed with this simple method could show the same excellent properties. Six electrodes were independently used to carry out the amperometric response of 5 mM glucose solution in order to reveal the reproducibility. The results were shown in Table 2. The relative standard deviation value was calculated to be 8.15%, which is compatible to the previous reports [20].

Conclusions

NPG membranes, a type of porous nanostructures, were fabricated by dealloying and were studied for glucose electrooxidation and detection. Taking advantage of the smallest pore size and largest active surface area, a-NPG exhibits the best activity and sensitivity toward the reaction both in neutral and alkaline conditions. The detection results in neutral media also promised that a-NPG exhibited excellent anti-interference from AA, urea, and sucrose at normal physiological levels and reproducibility characteristics. The a-NPG is thus expected to be a promising electrocatalyst for application in the fields of glucose electrochemical sensors and fuel cells.

Acknowledgment We thank Prof. Y. Ding and Houyi Ma for valuable discussions and sharing their nanomaterials and facilities.

References

1. Burke LD, Nugent PF (1997) Gold bull 30:43–53
2. Burke LD, Nugent PF (1998) J Electroanal Chem 444:19–29
3. Burke LD, Nuqent PF (1998) Gold Bull 31:39–50
4. Chen A, Holt-Hindle P (2010) Chem Rev 110:3767–3804
5. Chen A, Lipkowski J (1999) J Phys Chem B 103:682–691
6. Ding Y, Chen MW (2009) MRS Bull 34:569–576
7. Ding Y, Erlebacher J (2003) J Am Chem Soc 125:7772–7773
8. Ding Y, Kim YJ, Erlebacher J (2005) Adv Mater 16:1897–1900
9. Dong H, Cao XD (2009) J Phys Chem C 113:603–609
10. Erlebacher J, Aziz MJ, Karma A, Dimitrov N, Sieradzki K (2001) Nature 410:450–453
11. Ge XB, Wang RY, Cui SZ, Tian F, Xu LQ, Ding Y (2008) Electrochem Commun 10:1494–1497
12. Ge XB, Wang RY, Liu PP, Ding Y (2007) Chem Mater 19:5827–5829
13. Habrioux A, Sibert E, Servat K, Vogel W, Kokoh KB, Alonso-Vante N (2007) J Phys Chem B 111:10329–10333
14. Hsiao MW, Adzic RR, Yeager EB (1996) J Electrochem Soc 143:759–767
15. Huang JF (2008) Electroanalysis 20:2229–2234
16. Huang W, Wang MH, Zheng JF, Li ZL (2009) J Phys Chem C 113:1800–1805
17. Jia FL, Yu CF, Ai ZH, Zhang LZ (2007) Chem Mater 19:3648–3653
18. Jia F, Yu CF, Deng KJ, Zhang LZ (2007) J Phys Chem C 111:8424–8431
19. Kerzenmacher S, Ducre'e J, Zengerle R, Stetten FV (2008) J Power Sources 182:1–17
20. Lee YJ, Park JY (2010) Sens Actuators B: Chem. doi:10.1016/j.snb.201011037
21. Li YY, Ding Y (2010) J Phys Chem C 114:3175–3179
22. Li Y, Song YY, Yang C, Xia XH (2005) Electrochem Commun 9:981–988
23. Liu ZN, Huang LH, Zhang LL, Ma HY, Ding Y (2009) Electrochim Acta 54:7286–7293
24. Oesch U, Janata J (1983) Electro chim Acta 28:1237–1246
25. Park S, Chung TD, Kim HC (2003) Anal Chem 75:3046–3049
26. Vassilyev YB, Khazova OA, Nikolaeva NN (1985) J Electroanal Chem 196:127–144
27. Xu CX, Su JX, Xu XH, Liu PP, Zhao HJ, Tian F, Ding Y (2007) J Am Chem Soc 129:42–43
28. Xu CX, Wang LQ, Wang RY, Wang K, Zhang Y, Tian F, Ding Y (2009) Adv Mater 21:2165–2169
29. Ye JS, Wen Y, Zhang WD, Gan LM, Xu GQ, Sheu FS (2004) Electrochem Commun 6:66–70
30. Yuan JH, Wang K, Xia XH (2005) Adv Funct Mater 15:803–809
31. Zare HR, Habibirad AM (2006) J Solid State Electr 10:348–359
32. Zhang JT, Liu PP, Ma HY, Ding Y (2007) J Phys Chem C 111:10382–10388
33. Zhao CZ, Shao CL, Li MH, Jiao K (2007) Talanta 71:1769–1773
34. Zhou YG, Yang S, Qian QY, Xia XH (2009) Electrochem Commun 11:216–219